



[1], in this method the ratio between a selected voltage and a selected current, depending on the type of fault, is calculated to determine the distance to the fault. The second method is designated by automated fault location and diagnosis [2], in this method the recorded data at the relaying point is used to calculate the fault distance and fault locations at various laterals via their scenarios. Also, in this method, the inequalities of mutual coupling between phases can be taken into consideration. The third method is based on the reactive power flow [3], in which a selected phase or phases reactive power, depending on the type of fault, is divided by this particular phase or phases reactive power per unit length. In the fourth method updating current and voltage vectors with static load [1] are used to calculate the fault location with elimination of the effect load flow.

There are other techniques for feeder fed from two ends or for multi-infeed feeders such as Global Position Satellite (GPS) [4], synchronized data and unsynchronized data method [5], and method depends on Artificial Neural Networks ANNs [6].

In this paper, a comparative study among four fault location methods applied to a specific field medium voltage radial distribution feeder fed from one end is given. The comparison is carried out from the view point of accuracy, speed in determining the fault location and the ability of on-line application. Also, the effects of load current flow, fault distance from the source, system topology, fault resistance on the error of determining the locations for each method are investigated. The result will aid the field engineers to evaluate and select the most appropriate and accurate method for his own application. The specific feeder system used for this study is first simulated using EMTP as given below.

## II. SIMULATED SYSTEM

Feeder system used in this study is a typical medium voltage distribution feeder in Egyptian distribution network. This feeder is shown in Fig.1, in which the bus-coupler CB5 and isolator switch S1 are normally open. It is closed upon outages of one of main transformers. The locations of the distribution transformers along the feeder are as shown. The ratings of the transformers and other relevant parameters are as given in the appendix. In simulating this feeder the EMTP source type 14 is used and the PI-circuit branch representation is considered. The fault simulation was carried out for line-to-line and line-to-ground faults at equispace of 100 meters distant along the feeder, with normal operation (i.e. switch S1 and bus-coupler CB5 are open). This is carried out also with switch S1 closed and CB5 open which represent the worst condition as far as fault location is concerned. In the forgoing applications of the four fault location methods, the worst condition is considered.

Fault location is calculated from CB1 point to the fault point for each fault location methods compared. Samples of three-phase voltages and currents are given by EMTP simulation. The output of EMTP simulation is used as an input to a recursive discrete Fourier transform filters (DFTs) [7]. The output of these DFT represent the voltage and current signals at the relaying point. These

signals are used by the fault locator to compute the distance of the fault from the relaying point.

The algorithm of computation depends on the technique used as given in the subsequent sections.

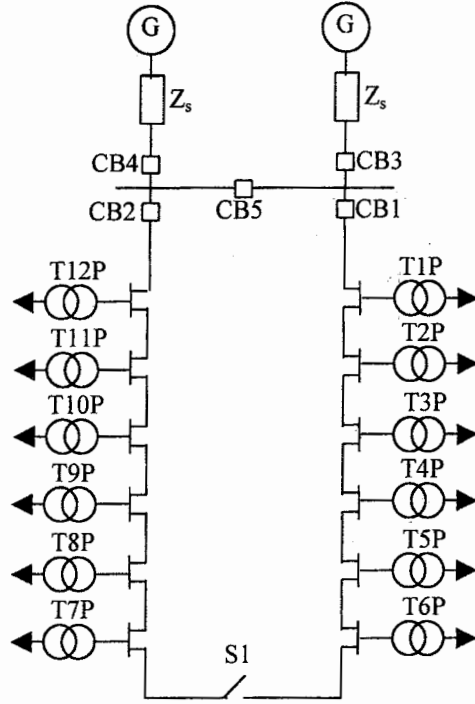


Fig. 1 Single line diagram of simulated system

### III. APPARENT IMPEDANCE METHOD

Apparent impedance seen by this fault locator is defined as the ratio between a selected voltage and a selected current phasors at CB1. this impedance represents the impedance from the CB1 point to the fault point and can be calculated as

$$Z_{app} = \frac{V_{select}}{I_{select}} = (r_1 + jx_1)D_c + \frac{I_{comp}}{I_{select}} R_f \quad (1)$$

where

$Z_{app}$  is the apparent impedance from the CB1 point to the fault point

$D_c$  is the computed distance from the relay point to the fault point

$r_1$  and  $x_1$  are the positive sequence resistance and reactance per unit length

$V_{select}$  is the selected voltage

$I_{select}$  is the selected current

$I_{comp}$  is the compensated current

The appropriate selected voltage and selected current phasors depends on the type of fault. For line-to-line faults, the selected voltage is the voltage difference of the two faulted phases and the selected current is the current difference of the two faulted phases (i.e. for line A-to-line B fault  $V_{select} = V_a -$

$V_b, I_{select} = I_a - I_b, V_{select} = V_a, I_{select} = I_a + kI_0$  and  $I_{comp} = 3I_0$  in line A and in line B due to fault. Double line to ground and three-phase faults are the same as line-to-line faults. However, for ground fault, the selected voltage is the voltage of the faulted phase and the selected current will be the faulted phase current in addition to a compensating factor (i.e. for line A-to-ground fault  $V_{select} = V_a, I_{select} = I_a + kI_0$ , and  $I_{comp} = 3I_0$  where  $kI_0$  is the compensating factor. This factor is to compensate for the effect of the fault resistance.

The percentage error of the fault location is computed at different points along the feeder, different values of fault resistance and at different loading conditions. In Fig.2a the percentage error is plotted against fault point distance for line-to-line fault with fault resistance  $R_f$  of 0, 10, and 20 Ohms. It can be seen that, with solid fault ( $R_f = 0$  Ohm), as the fault point is moved towards the end of the feeder the error is increased to about -7%. Also, for  $R_f = 10$  Ohm the error is increased at first towards a positive value of 5% then reduces to zero at the middle of the feeder. The error is increased again in the negative sense towards -8% at the end of the feeder. For  $R_f = 20$  Ohm, a similar pattern to the case of  $R_f = 10$  Ohm is obtain, but with higher values of error along the feeder. This result shows the significant effect of the position of fault along the feeder and the value of fault resistance on the fault locator estimation with this method.

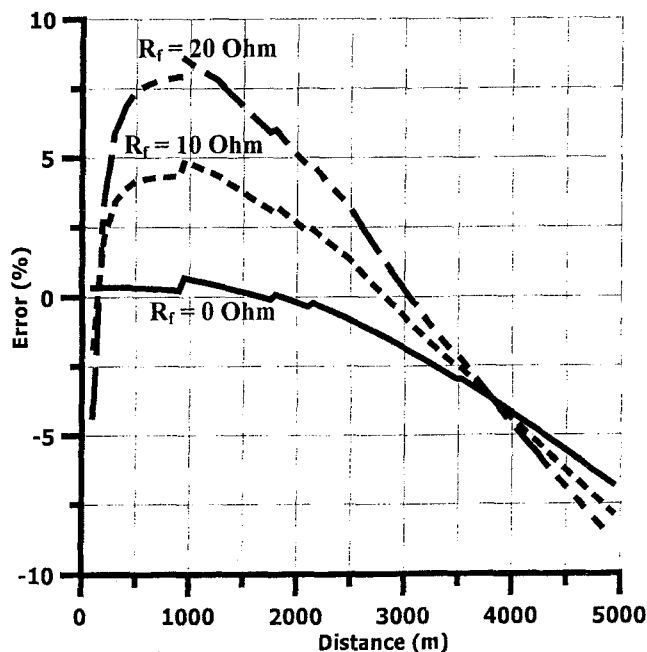


Fig.2a Fault location error along the feeder for different values of fault resistance for line-to-line fault with the first method.

The effect of load flow is examined with solid fault ( $R_f = 0 \text{ Ohm}$ ) for line-to-line fault and the results are plotted as shown in Fig.2b. It can be seen that as the load flow increases as the fault location error increases. The maximum error occurs at the end of the feeder at full-load of about  $-7\%$ . On the other hand at no-load the error is almost steady along the feeder to a less than  $+1\%$  regardless of the value of fault resistance.

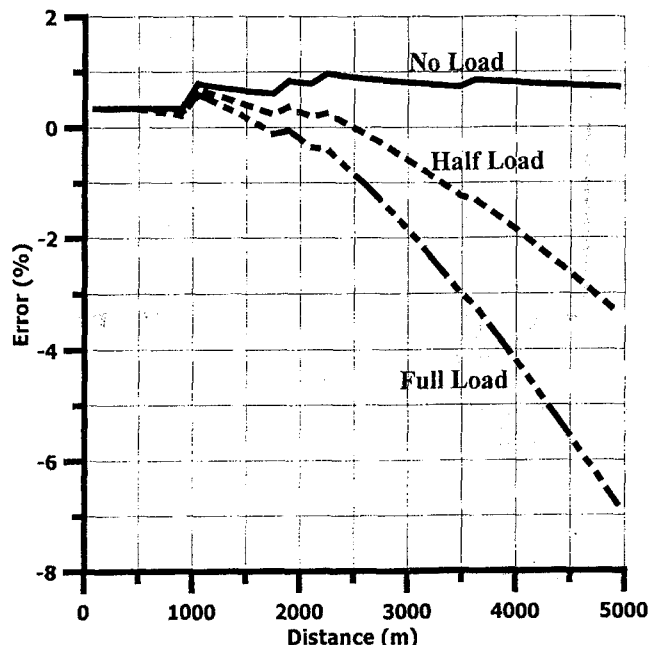


Fig.2b Fault location error along the feeder with different loading condition for line-to-line fault with the first method.

In Fig.3 the effect of same values of fault resistance on the error for line-to-ground fault is shown. It can be seen that, as the fault point is increased towards the end of the feeder the error proportionally increases to its maximum value (in the negative sense) at the end of the feeder. This pattern is obtained for all values of fault resistance. However, for the three values of fault resistance considered, the maximum error is obtained at the highest value of fault resistance ( $R_f = 20 \text{ Ohm}$ ) about  $-13.5\%$ . The effect of loading condition on the percentage of fault location error for line-to-ground fault is computed and in which the error also increases as the initial load flow increases. The maximum error also occurs at the end of the feeder of about  $-8.5\%$  at full-load.

#### IV. AUTOMATED FAULT LOCATION METHOD

In this method, distance to the fault point can be calculated using voltage and current phasors estimated at CB1 considering the effect of self and mutual impedances of the feeder, load type, and the fault type. Assuming equal self impedance and mutual impedance between phases, static load and line-to-line fault, distance to the fault point is computed, for phases a and b, from Eq.(2) as:

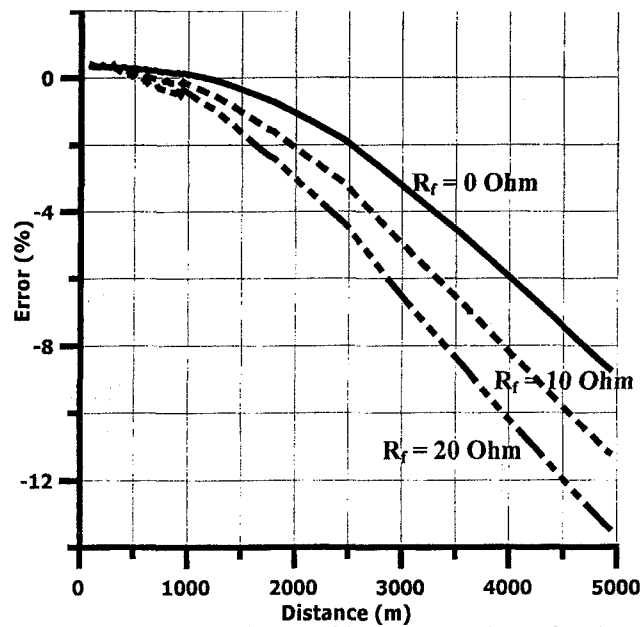


Fig.3 Fault location error along the feeder with different values of fault resistance for line-to-ground fault with the first method

$$V_a - V_b = D(z_s - z_m)(I_a - I_b) + (\Delta I_a - \Delta I_b)R_f \quad (2)$$

However for line-to-ground fault on phase a, fault distance is calculated from Eq.(3) as:

$$V_a = D(z_s I_a + z_m I_b + z_m I_c) + I_f R_f \quad (3)$$

where

$D$  is the distance from CB1 to the fault point.

$z_s$  is the self impedance.

$z_m$  is the mutual impedance.

$R_f$  is the fault resistance.

$\Delta I_a$  and  $\Delta I_b$  are the superimposed current in phase A and phase B respectively.

$I_f$  is the fault current.

The fault error was calculated along the feeder for  $R_f = 0, 10$  and  $20$  Ohms at full loading condition for line-to-line and line-to-ground faults. The results are plotted as shown in Fig.4a for line-to-line fault and in Fig.4b for line-to-ground fault. It can be seen that the error variation along the feeder, for line-to-line fault, has almost a similar pattern to the first method. However, the maximum positive error is at  $R_f = 20$  Ohms is about  $+7.0\%$  compared with about  $+8.5\%$  with the first method. The maximum errors at the feeder end has almost the same values of positive error as the first method. However, the pattern for line-to-ground fault is changed as shown in Fig.4b. in this figure, as  $R_f$  increases the percentage error increases and swings from positive to negative. It yields higher error than in the first method by values of about  $+4.0\%$  and  $-2.0\%$  at  $R_f = 20$  Ohms.

The initial load flow effect for line-to-line with solid fault is shown in Fig.5. It can be seen that the second method is affected by the initial load flow in a similar pattern to the first method.

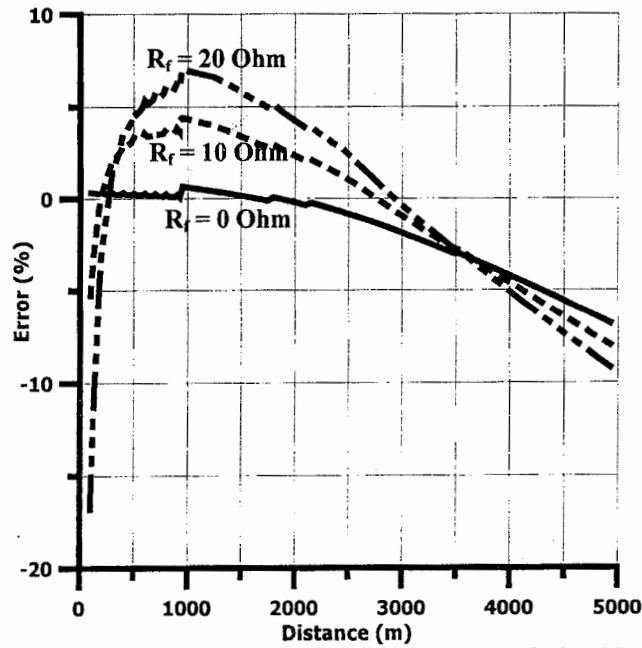


Fig.4a Fault location error along the feeder for line-to-line fault with different values of fault resistance with the second method

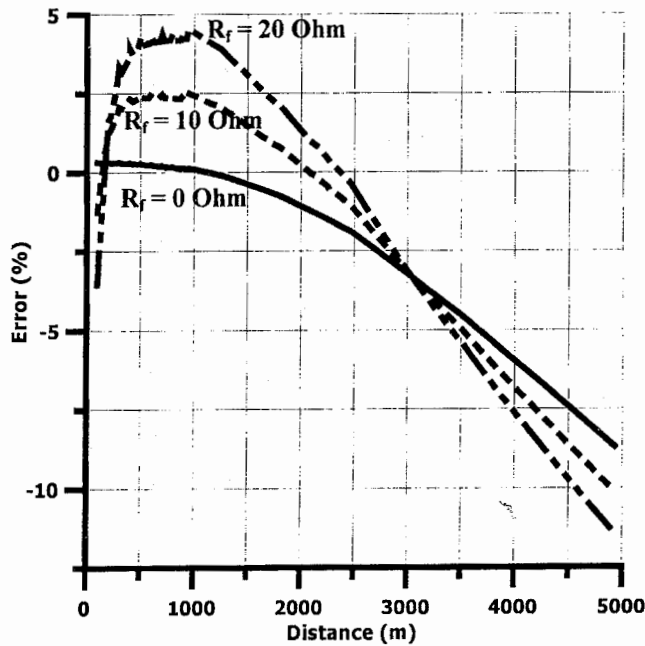


Fig.4b Fault location error along the feeder for line-to-ground fault with different values of fault resistance with the second method

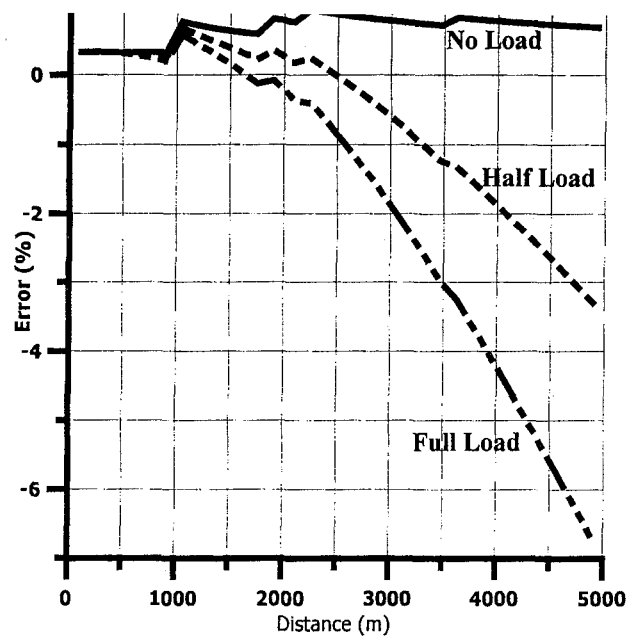


Fig.5 Fault location error along the feeder with different loading condition for line-to-line fault, with the second method.

### V. REACTIVE POWER METHOD

This method is mainly dependent on the selected phase or phases reactive power values. Therefore, it is assigned in this paper as reactive power method.

This method is a straight forward technique for determining fault location. Distance to the fault point can be defined as the ratio between the selected phase or phases reactive power flow in the distribution system to the selected phase or phases reactive power per unit length. These selected quantities are depending on the type of fault, for example in case of phase a-to-ground fault selected phase reactive power flow is equal to  $Q_a$ .

The effect of different values of fault resistance at full-load condition is shown in Fig.6a and Fig.6b, for line-to-line and line-to-ground faults respectively. It can be seen that the effect of varying  $R_f$  from 0 to 20 Ohms on the error is substantial.

Also, the effect of different loading conditions with solidly short circuit is shown in Fig.7 for line-to-line fault. In this figure, it can be seen that the maximum error at full-load at the end of the feeder is about -4.1%. This value is quit less than of those of the first and second methods. However, the effect of initial load flow for line-to-ground fault has almost the same pattern as that of the line-to-line fault.



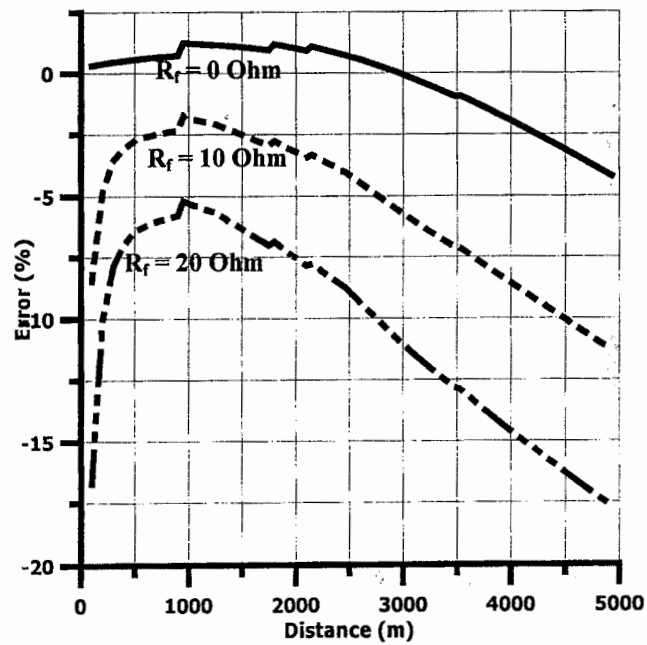


Fig.6a Fault location error along the feeder for line-to-line fault with different values of fault resistance with the third method

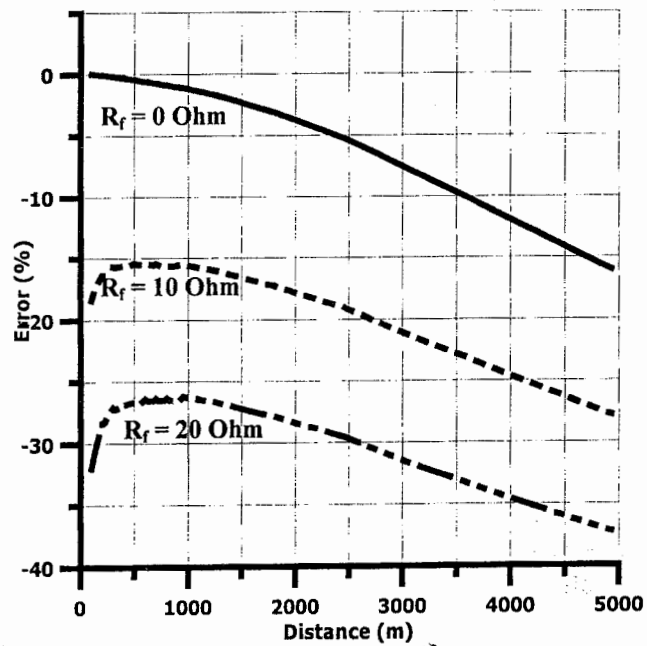


Fig.6b Fault location error along the feeder for line-to-ground fault with different values of fault resistance, with the third method

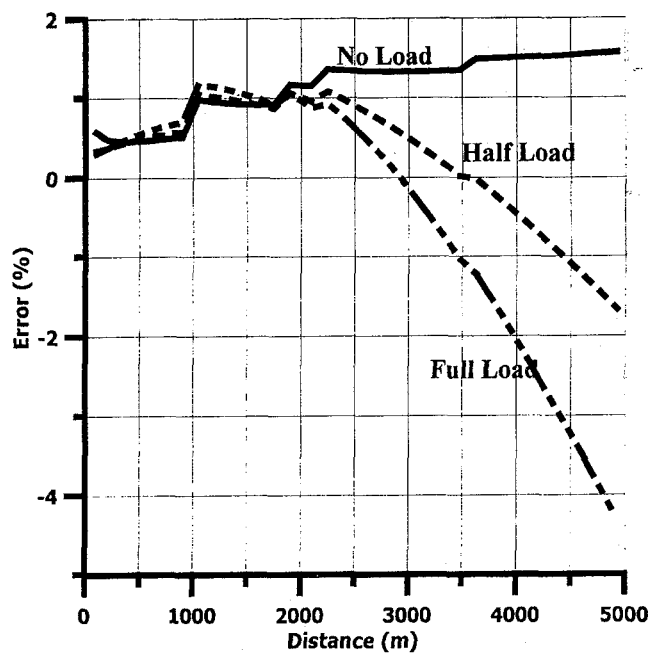


Fig.7 Fault location error along the feeder with different loading condition for line-to-line fault, with the third method.

### VI. UPDATING VOLTAGE AND CURRENT METHOD

In this method, distance to the fault is calculated as mentioned in the apparent impedance method which uses voltage and current at substation, but in this method voltage and current are shifted to the load buses. First, distance is calculated using voltage and current measured at substation via apparent impedance, if this distance is greater than the length of the first section, voltage and current computation will be shifted to the first load bus and distance is calculated again, and so on. From shifted voltage and load characteristic, load current will be calculated precisely and hence its effect on the calculated distance can be eliminated.

The results of fault location errors, calculated by this method along the feeder for line-to-ground fault and with  $R_f = 0, 10, 20\text{Ohms}$  are as shown in Fig.8. In this figure it can be seen that the error is below +0.34% and remains almost constant along the feeder. Also, variation of  $R_f$  has no effect on the error beyond a distance of 1500 meter. However, the error is increased relative as the fault location is decreased below 1500 meter. These results are similar to those obtained with no-load cases. Similarly for line-to-line fault, there is no significant of the value of  $R_f$  on the error along the feeder.

### VII. COMPARISON OF THE RESULTS

Fault location error against the fault location along the feeder is plotted for each of the four methods at  $R_f = 10\text{ Ohms}$  and at full-load as shown in Fig.9a for line-to-line fault and Fig.9b for line-to-ground fault. From these figures, it can be seen that in the first, second and third methods fault location error is increased as the fault point moves towards the end of the feeder. However, in the fourth methods the error is steady along the feeder and less than 1.0% with

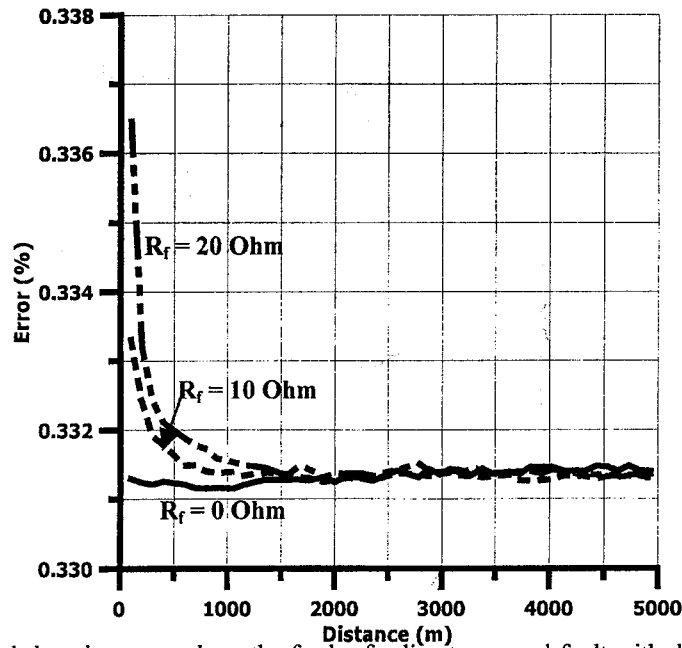


Fig.8 Fault location error along the feeder for line-to-ground fault with different values of fault resistance, with the fourth method

both line-to-line or line-to-ground fault. This mainly because the effect of load current flow is taken care of. In the first and second method a maximum error at the end of the feeder of about  $-8.0\%$  for line-to-line fault and about  $-11.0\%$  for line-to-ground fault. The third method is the most affected by the type of the fault as it yields a maximum error of about  $-11.0\%$  for line-to-line fault and about  $-27.0\%$  for line-to-ground fault. It can also concluded, increasing  $R_f$  increases the resultant error. This increase in error is emphasized as the initial load current flow increases. On the other hand decreasing the initial load flow improves the accuracy of fault location determination. The higher accuracy is obtained at no-load, where variation of  $R_f$  has no effect, with all four methods.

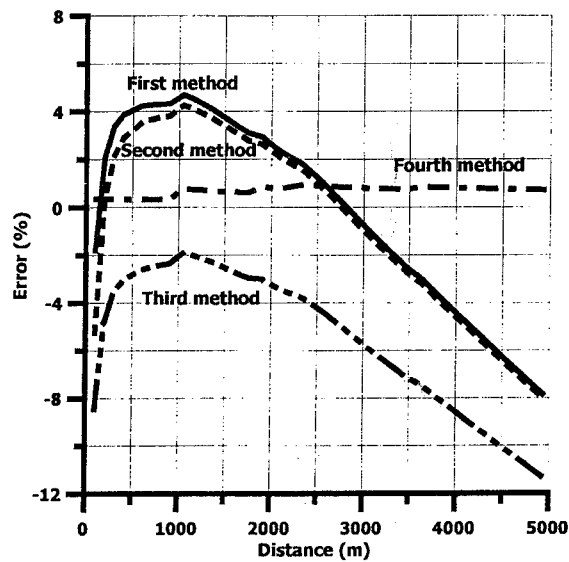


Fig.9a Fault location error along the feeder for line-to-line fault for the four methods with fault resistance  $R_f = 10 \text{ Ohm}$

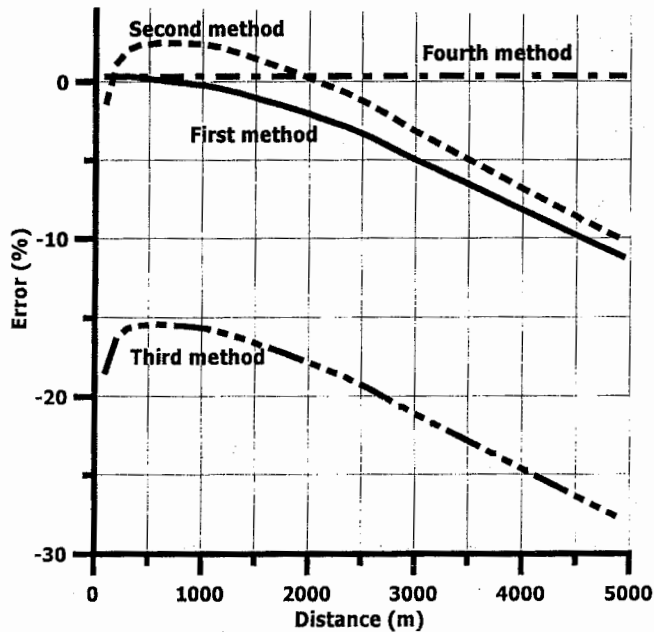


Fig.9b Fault location error along the feeder for line-to-ground fault for the four methods with fault resistance  $R_f = 10$  Ohm

Response of the algorithm of each of the four methods was examined for a sudden application of line-to-ground fault at 2000 meter from CB1 on the feeder. The results are plotted as shown in Fig.10, in which a steady output is obtained after about 15 msec from the instant of fault application. This response may not be adequate for on-line fault location determination application, if the fault is detected by instantaneous relays. However, with definite or inverse time relays, this response is quite adequate for most practical applications.

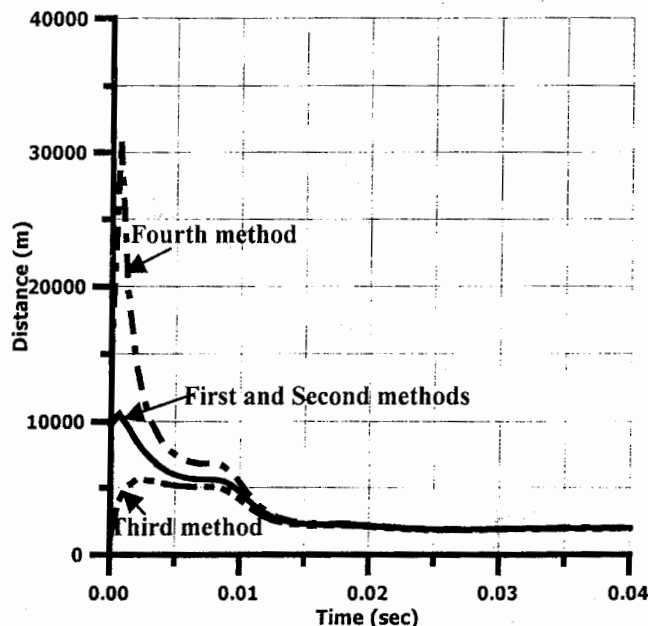


Fig.10 Response of the four method algorithms for a sudden application of line-to-ground fault at 2000 m from CB1

## VIII. CONCLUSION

A comparative study among four fault location methods, used in distribution systems, has been presented. The results have shown that with the first three methods considered, the percentage error of fault location increases as the initial load flow increases and as the fault location moves away from the relaying point. Also increasing of fault resistance have had substantial effect on increasing the error particularly with high values of load current flow. The fourth method has provided the smallest error, amongst the four methods, along the feeder. Providing the initial load flow at various tapping is known. In the first and second methods the line-to-ground fault has yielded an error of about 2.0% to 4.0% more than the line-to-line fault at rated full-load flow. The third method, however is substantially affected by the type of fault, as an error difference of about 16.0% is obtained at full-load. In all four methods a steady output from the fault locator is obtained in about 15 msec from the instant of fault application. This is adequate response for on-line applications. The four methods fail to distinguish between the lateral and main feeders fault locations. However, this distinction may be obtained if the protective devices placement and scenarios of their time-current behavior are known.

## REFERENCES

- [1] Adly A. Girgis, Christopher M. Fallon, David L. Lubkeman, "A Fault Location Technique for Rural Distribution Feeders," IEEE Transactions on Industry Applications, Vol. 29, No. 6, November 1993, pp. 1170-1175.
- [2] Jun Zhu, David L. Lubkeman, and Adly A. Girgis, "Automated Fault Location and Diagnosis on Electric Power Distribution Feeders," IEEE Transactions on Power Delivery, Vol. 12, No. 2, April 1997, pp. 801-809.
- [3] T. Takagi et al., "Development of a New Type Fault Locator Using One Terminal Voltage and Current Data," IEEE Trans. Power App. Syst. Vol. PAS-101, No. 8, pp.2892-2898, Aug. 1980.
- [4] Harry Lee, Abdul M. Mousa, " GPS Traveling Wave Fault Locator Systems: Investigating into the Anomalous Measurements Related to Lighting Strikes," IEEE Transactions on Power Delivery, Vol. 11, No. 3, July 1996, pp. 1214-1223.
- [5] Adly A. Girgis, David G. Hart, William L. Peterson, "A New Fault Location Technique for Two-and Three-Terminal Lines," IEEE Transactions on Power Delivery, Vol. 7, No. 1, January 1992, pp. 98-107.
- [6] Zhihong Chen and Jean-Claud Maun, "Artificial Neural Network Approach to Single-Ended for Transmission Lines," IEEE Transactions on Power System, Vol. 15, No. 1, February 2000, pp. 370-375.
- [7] Murty V.V.S.Yalla, " A Digital Multifunction Protective Relay," IEEE Transactions on Power Delivery, Vol. 7, No. 1, January 1992, pp. 193-200.

## APPENDIX

The parameters of the simulated system are given as:

Source impedance ( $Z_s$ ) is 0.05 p.u. on 200 kVA, 11 kV base.

The main feeder is underground cable of:

Self impedance  $Z_s = 0.1324 + j1.0713$  Ohm/km  
= 0.1324+j1.0713 Ohm/km

The distribution transformer ratings and their location distances from CB1 are as given in table 1 below:

*Table 1. Transformer ratings and location*

Transformer designation	Rating kVA	Distance from CB1 (m)
T1P	250	300
T2P	200	500
T3P	500	950
T4P	500	1250
T5P	250	1450
T6P	500	1650
T7P	300	2300
T8P	500	2315
T9P	300	2326
T10P	200	2526
T11P	500	3376
T12P	300	4126

## " دراسة مقارنة لطرق تحديد الخطأ في نظم التوزيع الإشعاعية "

أ.د. عبدالمقصود إبراهيم تغلب ، د. حاتم عبدالسميع درويش

قسم الهندسة الكهربائية - كلية الهندسة - جامعة المنوفية

أ.د. محمد الحازندار ، أ.د. جمال السعيد ، م. محمد علم

قسم هندسة القوى الكهربائية - كلية الهندسة - جامعة طنطا

### ملخص المقالة

تقدم المقالة دراسة مقارنة بين أربع طرق عددية تستخدم لتحديد مكان العطل في شبكات التوزيع الإشعاعية والمغذاة من جانب واحد. وترجع أهمية هذه المقالة لما في التحديد السريع لمكان الأعطال من فوائد مهمة في رفع نسبة العزل بالشبكات والاعتمادية عليها. ولقد تمت دراسة تأثير دقة هذه الطرق بعدة عوامل منها: قيمة مقاومة الخطأ، بعد نقطة الخطأ عن المصدر (لوحة التوزيع)، نوع الخطأ، وقيم الأحمال. واستخدمت الدراسة في نمذجة شبكة التوزيع برنامج المحاكاة E MTP والذي استخدم في تمثيل إحدى الحلقات الفعلية وأحد الخطوط الهوائية بشركة كهرباء مصر الوسطى. واستخدمت مخرجات برنامج المحاكاة من جهود وتيارات كمدخلات لمرح فورير الرقمي لاستنتاج القيم المتجهة خم في الثلاثة أوجه وعلى أساس القيم المحسوبة من فورير يتم حساب مكان الخطأ باتباع خوارزم أربع طرق مختلفة لإتمام المقارنة. وتشمل هذه الطرق:

١- طريقة المعاوقة الظاهرية

٢- طريقة اكتشاف العطل المميكن

٣- طريقة القدرة الغير فعالة

٤- طريقة المعاوقة الظاهرية المعدلة

وأوصت الدراسة بعد قياسات ونتائج مقارنة متعددة بالطريقة الرابعة وهي المعاوقة الظاهرية المعدلة ولذلك لتمييزها في تحديد أفضل لمكان الخطأ تحت الظروف المختلفة للكابلات الأرضية. كما تبين أيضا عجز الطرق الأربع عن تمييز مكان العطل بين تفرعات الخطوط الهوائية وذلك لتمثيل حالة الخطأ بما والتي يمكن التغلب عليها باستخدام تقنيات الاتصال بين عناصر النظام خصوصا عند التفرعات. وتبين أيضا أن استحابة هذه الطرق تحتاج على الأقل إلى ١٥ مللي ثانية من بيانات الجهد والتيار للمعدى من لحظة حدوث الخطأ حتى تبدأ المسافة المقدرة بما معبرة عن مكان العطب.